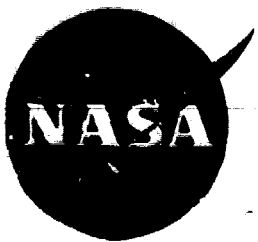# General Disclaimer

One or more of the Following Statements may affect this Document

- This document has been reproduced from the best copy furnished by the organizational source. It is being released in the interest of making available as much information as possible.

- This document may contain data, which exceeds the sheet parameters. It was furnished in this condition by the organizational source and is the best copy available.

- This document may contain tone-on-tone or color graphs, charts and/or pictures, which have been reproduced in black and white.

- This document is paginated as submitted by the original source.

- Portions of this document are not fully legible due to the historical nature of some of the material. However, it is the best reproduction available from the original submission.

NASA CR-135031

INVESTIGATION OF METAL HYDRIDE MATERIALS AS

HYDROGEN RESERVOIRS FOR METAL-HYDROGEN BATTERIES

by Michael Onischak

ENERGY RESEARCH CORPORATION

prepared for

NATIONAL AERONAUTICS AND SPACE ADMINISTRATION

INVESTIGATION OF METAL HYDRIDE MATERIALS AS

HYDROGEN RESERVOIRS FOR METAL-HYDROGEN BATTERIES

Michael Onischak

ENERGY RESEARCH CORPORATION

3 Great Pasture Road

Danbury, Connecticut 06810

prepared For:

NASA LEWIS RESEARCH CENTER

21000 Brookpark Road

Cleveland, Ohio 44135

Contract NAS3-18557

Dr. Marvin Warshay, Project Manager

Date: June 30, 1976

TABLE OF CONTENTS

TABLE OF CONTENTS
(continued)

LIST OF FIGURES

LIST OF TABLES

ABSTRACT

The performance and suitability of various metal hydride materials were examined for use as possible hydrogen storage reservoirs for secondary metal-hydrogen batteries.

Lanthanum pentanickel hydride appears as a probable candidate in terms of stable hydrogen supply under feasible thermal conditions.

A kinetic model describing the decomposition rate data of the hydride has been developed.

INVESTIGATION OF METAL HYDRIDE MATERIALS AS

HYDROGEN RESERVOIRS FOR METAL-HYDROGEN BATTERIES

1. SUMMARY

Important performance characteristics of metal hydride materials were evaluated for application as hydrogen storage reservoirs for secondary metal-hydrogen batteries.

Among the four probably hydride materials examined, lanthanum pentanickel appears as the most likely candidate for integration into a metal-hydrogen battery. Its hydrogen supply rate during the battery discharge is sufficient over a wide range of temperatures. It exhibits the greatest tolerance of the gaseous environment of the battery.

The other three hydride materials evaluated were iron-titanium, vanadium, and columbium.

An experimental method was devised to obtain isothermal rate data of hydride decomposition. A kinetic model for the decomposition rate of lanthanum pentanickel was developed. It presents an excellent qualitative description of all the aspects of the data. An approximate first order rate constant was obtained and compares well with data in the literature. Quantitative fitting of the model requires more data than was taken in this initial study. The model can be applied to describe other hydrides' suitable data of decomposition rates under isothermic conditions.

An unsteady state analysis of the heat transfer between a typical nickel-hydrogen battery and lanthanum pentanickel hydride was done during discharge. The results indicate that the endothermic lanthanum pentanickel would not be thermally limited.

2. INTRODUCTION

The purpose of this study was to investigate the performance characteristics of metal hydride forming materials to determine their suitability as hydrogen storage reservoirs in metal-hydrogen batteries[1,2,3].

The performance characteristics involve the hydrogen stor-

age capacity and the rates of hydrogen pickup and release as
well as the compatibility with metal-hydrogen batteries. The
thermal behavior of integrated hydride-battery systems and the
modeling of the hydrogen supply rate were also examined.

Metal-hydrogen secondary batteries such as nickel-hydrogen
(or silver-hydrogen) are created by the combination, for in-
stance, of a secondary nickel oxide electrode of the type that
is used in nickel-cadmium batteries and a hydrogen gas diffusion
electrode of the type used in fuel cells.

Upon charging the nickel-hydrogen battery, the nickel hy-
droxide is converted to its charged state and on the surface of
the hydrogen electrode, hydrogen gas is evolved. This gas must
be stored for subsequent use in the discharge of the battery.

In void volume storage of typical batteries the hydrogen
gas storage pressure reaches approximately 3.55×10^6 pascals
(35 atm). With hydride storage, this maximum pressure can be
reduced to about 3×10^5 pascals (3 atm).

The take-up, storage, and release of the hydrogen gas by
the metal hydride materials with respect to the operation and
environment of metal-hydrogen batteries is primarily what this
study is to characterize and evaluate. An application for
metal-hydrogen batteries is in satellite power systems. A typ-
ical duty cycle for the battery is presented in Appendix 1.

Specifically, this study was concerned with the character-
ization of four possible metal hydride materials that could
operate in the specified temperature range of 0 to 50°C. These
materials are vanadium, columbium (niobium), iron-titanium, and
lanthanum pentanickel.

3. MATERIAL CHARACTERIZATION

Qualitative and quantitative analysis were made on each
hydride material prior to testing. The major metal constituents
and the major and minor impurities were identified using the
methods of standard wet chemistry, X-ray spectrometry, and emis-
sion spectrography. Combined oxygen, nitrogen, and carbon were
analyzed at an independent laboratory using an inert gas fusion
apparatus.

The materials, vendors and vendor specifications are pre-
sented in Table 1. The results of the analysis of the materials
are presented in Table 2.

The analysis of each candidate material prior to testing can

2

TABLE 1 MATERIAL AND VENDOR SPECIFICATION

	Material	Formula	Vendor and Specification	
1.	Lanthanum Pentanickel	$LaNi_5$	Ronson Metals Corp.	67.5%Ni, 32.2%La, single phase, crushed alloy
2.	Lanthanum Pentanickel	$LaNi_5$	Molybdenum Corp. of America	68%Ni alloy
3.	Iron-Titanium	FeTi	National Lead Co.	(sample from Brookhaven National Lab.)
4.	Iron-Titanium	FeTi	Dayton Research Institute	53.83%Fe, 46.17%Ti
5.	Vanadium	V	Atomergic Chemetals Company	99.9% dendritic crystals
6.	Columbium (niobium)	Cb	Atomergic Chemetals Company	99.8% metal pellets (200 mesh)
7.	Vanadium Hydride	VH	Atomergic Chemetals Company	nuclear grade
8.	Columbium Hydride	CbH	Atomergic Chemetals Company	nuclear grade

TABLE 2 MATERIAL ANALYSIS

MATERIAL	MAJOR CONSTITUENTS (wgt %)	MINOR CONSTITUENTS (wgt %)											
		Co	Al	Bi	Cu	Fe	Mn	Pb	Si	Ag	Ti	Cr	O_2
LaNi$_5$ No. 1	67.49% Ni, 32.15% La	<.001	<.001	<.001	.005	.01	.001	.001	.001	<.001	<.001	<.001	130ppm
2	64.37% Ni, 31.28% La	.03	.04	<.001	.05	.01	.001	.01	.05	.001	<.001	.02	2.7

MATERIAL	MAJOR CONSTITUENTS (wgt %)	Al	Si	Ge	Mo	Ni	V	Sn	Cu	Mg	
FeTi No. 3	54.08% Fe, 43.14% Ti	<.001	.005	<.001	.001	.001	<.001	.005	.002	.003	3600ppm
4	53.95% Fe, 44.01% Ti	<.001	<.001	<.001	<.001	<.001	<.001	<.001	.005	.002	390ppm

MATERIAL	MAJOR CONSTITUENTS (wgt %)	Al	Si	Ge	Fe	Mo	Ni	Ti	V	Sn	Cu	Mg
V No. 5	99.90% V	<.001	.010	<.001	<.001	<.001	<.001	<.001	Maj	.001	<.001	.001
Cb No. 6	99.8% Co	<.001	.001	<.001	<.001	<.001	<.001	<.001	<.001	.008	<.001	.001
VH No. 7	98.61% V	<.001	.01	<.001	<.001	<.001	<.0011	<.001	Maj	.001	.001	.001
CbH No. 8	98.60% Cb	<.001	.01	<.001	<.001	<.001	<.001	<.001	<.001	.01	<.001	.001

4

provide information about composition which may be useful in correlating perf' nance variations. In this study, the purest materials available were used in performance evaluation.

In general, except for oxygen combined in the materials, no other measured minor constituent could be seen to significantly alter the behavior of the hydride materials. The analyzed presence of carbon and nitrogen could not be seen to significantly alter performance.

Certain hydride materials such as vanadium or columbium are known to be sensitive to certain impurities or trace additives. ([4],[5]). The impurities, mostly other metals, alter the dissociation pressures of the hydride. In some cases, crucible contamination during production of the hydride material could be a significant factor in reducing hydrogen capacity. Typically, these contaminants would appear as aluminum and silicon present in about ten times the normal impurity level.

4. PERFORMANCE CHARACTERIZATION

1. General Background

A successful hydride material as a hydrogen reservoir for a metal-hydrogen secondary battery has to perform within certain specifications and restrictions.

The hydride/battery system's electrical performance cannot be limited by the metal hydride's capacity, its formation (charging) rate, or its decomposition (discharging) rate. Also its cycle life and resistance to the battery environment are important. All of these aspects must be known in the battery's operating temperature range of 0 to 50°C.

The four particular candidate hydride materials were selected because in the temperature range of interest, their storage pressures do not exceed five atmospheres.

The necessary equipment was constructed to measure the equilibrium pressure-composition-temperature (P-C-T) behavior and capacity, the rate of hydride formation and decomposition, and the cyclic hydriding behavior in various hydrogen environments.

5

The equilibrium capacity of the metal hydride is important and relates to battery capacity. hydride weight and pressure levels. The intrinsic rates of formation and decomposition of the metal hydride should not be below the battery's use rate. The repeated cycling ability of the hydride materials should match that of the battery's.

Other characteristics that are important to hydride/battery design are the heats of hydride decomposition and energy of activation. The activation of the metal hydride and its handling characteristics are also important in selecting the hydride material.

2. Apparatus Description

   a. Equilibrium Pressure-Composition-Temperature (P-C-T) Apparatus

The apparatus for obtaining the P-C-T behavior of the hydride materials in the 0 to 50°C temperature range is shown schematically in Figure 1. The equipment measures the amounts of hydrogen given-off and taken-up by a given sample of metal hydride at a given temperature and at the corresponding pressure. The moles of hydrogen transferred are simply estimated by measuring the pressure changes in a known volume tank held at constant temperature.

The sample of the hydride material, usually five to ten grams, is held in a small volume cylinder, about 20-30cm^3. The hydride is activated in this vessel in a separate activation apparatus and then transferred to the equilibrium apparatus. A sample vessel shut-off valve prevents hydrogen loss or contamination. The P-C-T apparatus is then evacuated, purged with helium, evacuated, and filled with hydrogen before the sample valve is opened. The hydrogen gas used in all tests was purchased to a purity of 99.995% or better.

In the sample vessel, stainless steel balls of 1.59 mm and 3.18 mm diameter were dispersed with the hydride material. These increased the heat capacity and heat conduction through the powdered hydride material to aid in maintaining isothermal conditions. The entire sample holder including a large two micron sintered stainless steel filter was immersed in a stirred water bath. Thermocouples inside the cylinder, on the outside wall, and in the water bath monitored the temperature.

A large calibrated volume cylindrical tank (about 2.6 liters) was used to collect the hydrogen released by the hydride from the small volume cylinder. The sample holder and its connecting tubing and valves amount together to slightly less
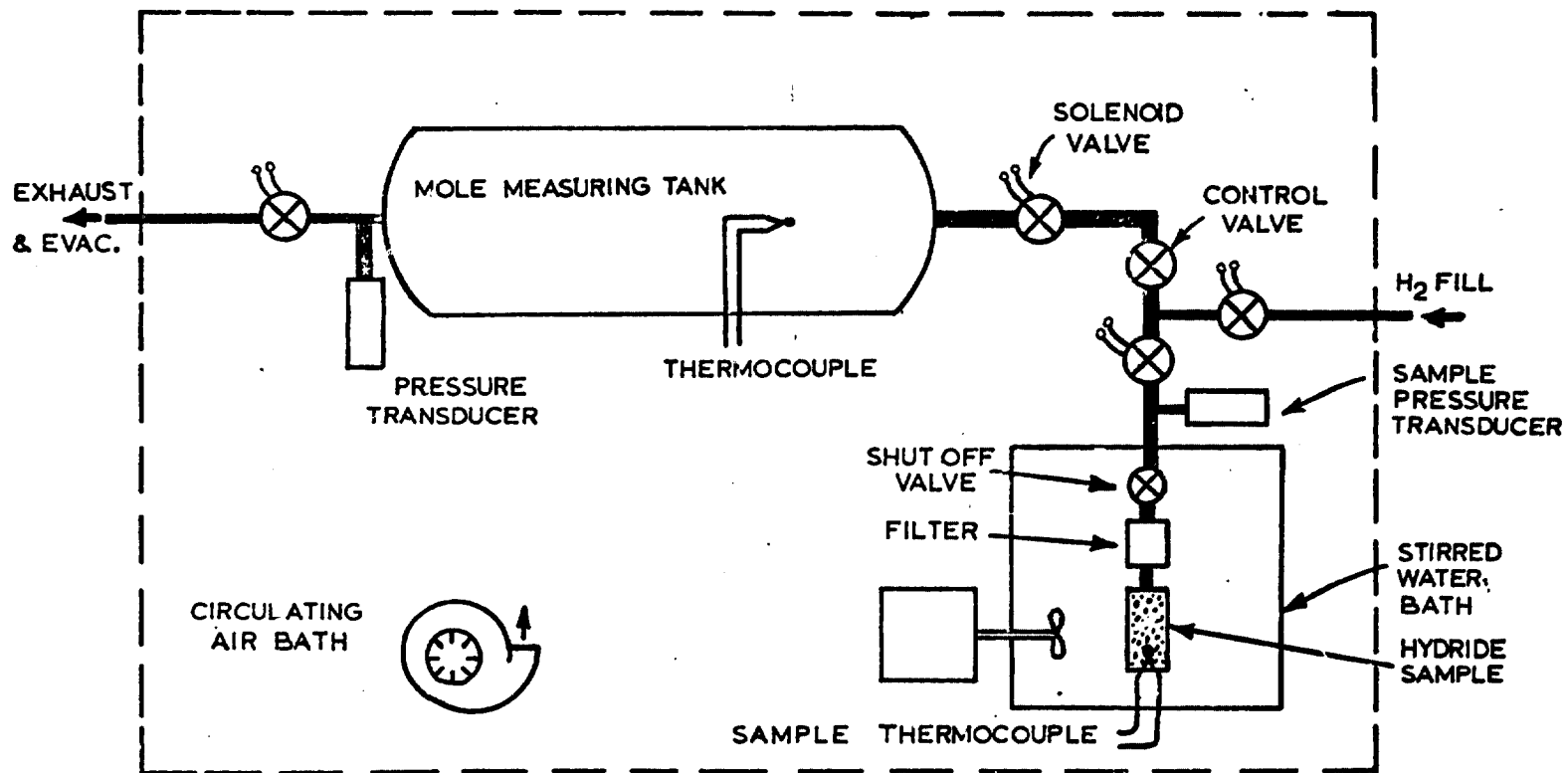
6

FIGURE 1   SCHEMATIC DIAGRAM OF P-C-T AND RATE APPARATUS

than 3% of the volume of the large tank.

The large tank, tubing and valves were all enclosed in a large insulated box that formed the controlled air bath. The tank temperature could be maintained within ± 2°C during the duration of experimentation, and within ± 0.1°C during any one collection of hydrogen. Thermocouples inside and outside the tank monitored the temperature.

The moles of hydrogen in the tank were estimated using the ideal gas law, knowing the volume and temperature, and measuring the pressure in the tank. The tank and sample pressures were measured with pressure transducers accurate to ± 0.1%. Digital readout meters and chart recorders were used to read the pressures.

Equilibrium was allowed to establish before and after hydrogen transfers for periods of several hours until no pressure or temperature changes were detected. Small amounts of hydrogen were collected at any one time in discharge periods up to 30 seconds. The sample container was then closed and allowed to re-equilibrate. In this way the pressure-composition isotherm was constructed over the range of hydride composition.

b. Metal-Hydride Rate Apparatus

The apparatus used to measure the isothermal rates of hydride decomposition is the same P-C-T apparatus shown in Figure 1 but operated in a different manner. The difference is that the time of hydrogen discharge into the tank is kept very short (∿ 10 seconds) and the measured pressure rise in time in the measuring tank gives the estimate of the rate.

The very short discharge time permits the maintenance of isothermal conditions of the hydride sample. The thermocouple inside the sample vessel did not vary more than 1°C in the 10-15 seconds of discharge.

The overall transfer rate is calculated from the change in moles of hydrogen in the tank during the time interval of hydrogen transfer. Using the ideal gas law, the change of pressure in the constant volume, constant temperature tank represents the moles of hydrogen entering the tank.

The increase in moles of hydrogen in the tank in the short discharge time was easily obtained from the slope of straight rising pressure lines on a chart recorder. The chart record showed an initial jump to a higher pressure level in less than 1 second (representing the void volume equilibration between vessels) which was followed by a constant rising pressure in the

8

remaining 10 seconds. Beyond 10 or 15 seconds the straight line pressure rise would cease and produce a curve. At this point the hydride was beginning to cool by several degrees.

The overall rate of isothermal decomposition is thus obtained from a series of short time discharges from the sample holder into the mole measuring tank. The overall rates can be measured over the 0-50°C range of this study by maintaining the temperature of the sample holder.

Also, the parameter of backpressure in the tank as seen by the sample can be varied to study this effect and yield intrinsic rates at near zero backpressure. The hydrogen backpressure in the tank can be varied from zero to the isotherm equilibrium pressure. The change in tank backpressure during the short discharge times was very small; the maximum pressure rise in the tank was about 2.07×10^4 pascals (0.2 atm) with the extreme situation of vacuum initially in the tank and the lanthanum pentanickel hydride hydrided fully at 2.21×10^5 pascals (2.2 atm).

c. Hydride Cycling Apparatus

The ability of the hydride materials to pickup and release hydrogen repeatedly was tested in various forms of a cycling apparatus shown schematically in Figure 2A and B. The cycling performance was conducted and measured under three different conditions. One cycling apparatus tested the hydriding and dehydriding with pure, dry hydrogen. Another tested the cycling performance with pure hydrogen gas saturated with water. The third cycling test involved the hydride operating in a two amp-hour nickel-hydrogen test battery. Here the effects of the actual environment of the battery during charge, discharge and stand were examined. The combination of the results show directly and indirectly the effect on cycle life of various components present in a battery environment.

The dry hydrogen cycling apparatus shown in Figure 2A involved simply a 20cc sample holder and timer-controlled solenoid valves directing fresh hydrogen to the sample, and exhaust hydrogen out of the sample. The sample holder was immersed in a room temperature water bath. The flow rates of hydrogen in and out were set such that the filling or discharging were about 80% completed in the 30 minutes each solenoid valve was open. Exhaust tubing was made rather long to reduce back diffusion of oxygen and room gases. About 80 to 85% of the hydrogen in the hydride was transferred in the 30 minute periods. Periodically, the exhausted hydrogen was collected to record capacity against cycle number.
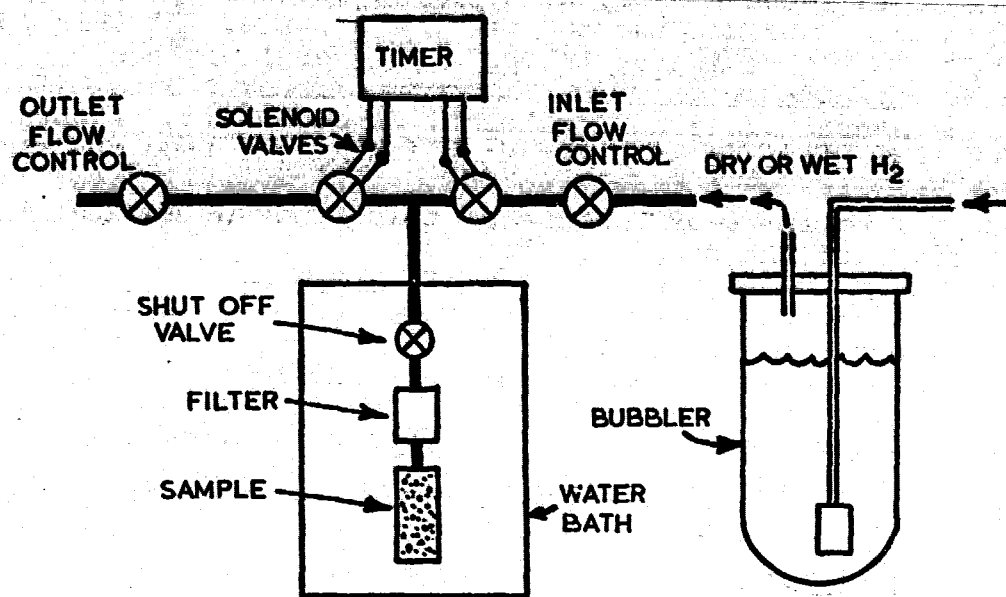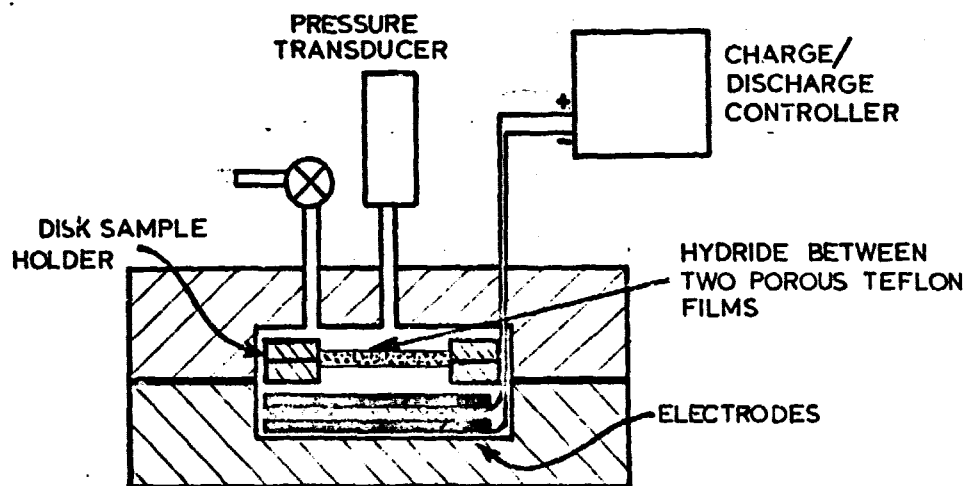
FIGURE 2A   DRY & WET HYDROGEN CYCLING APPARATUS

FIGURE 2B   NICKEL-HYDROGEN TEST BATTERY CYCLING APPARATUS

10

The wet hydrogen cycling apparatus was identical to the dry apparatus except that the hydrogen went through a high pressure bubbler before contacting the hydride. In this way a certain amount of water vapor (14°C dew pt) was introduced. The apparatus was operated in the same manner as the dry cycler.

The third cycling performance apparatus shown in Figure 2B contained several electrodes forming a 2 amp-hour nickel-hydrogen battery that was operated with the hydrogen stored and released by the metal hydride.

In a heavy-walled stainless steel cylindrical test vessel, several disk-shaped electrodes were placed under a disk-shaped hydride sample holder. The holder was simply two doughnut shaped plastic disks that captured two circular sheets of porous Teflon film. The hydride material was held between the films. The porous Teflon film allowed gas passage but prevented any liquid passage, such as condensed water vapor cr electrolyte.

This sandwich disk hydride holder was positioned on one side of the hydrogen electrodes. This produced a very short heat transfer path between the hydride and the electrodes. The void volume of the cell was determined with helium to be about 82cc.

The operation of this battery was controlled by an automatic charge and discharge controller. The cyclic operation was divided between 4 hours of charge at 0.6 amps and 4 hours of discharge at 0.5 amp. This cycle allows sufficient time for heat dissipation so that the heat transfer rate would not control the hydride pickup and release of hydrogen. Also this test was designed to be limited by the capacity of the hydride, not by the active nickel compound in the nickel electrode. In this way the performance of the total unit is dependent directly on the performance of the hydride.

The real environment for the hydride in a battery contains water vapor of the battery plus some oxygen which is produced near the end of charge. The oxygen produced during overcharge at the positive electrode surface is recombined without any difficulties at the hydrogen electrode.

3.   Experimental Results

    a.   Initial Cycling Tests

Various cyclic performance tests of the candidate materials showed in early stages that some materials would probably be unsuitable in operation in conjunction with a metal-hydrogen battery environment. Henceforth, to use the program time most effectively and not to reproduce information in the literature

not all hydride materials were tested in all aspects of this program.

One important point about the environment in a metal-hydrogen battery developed. The bulk of the hydrogen atmosphere in the battery always will contain water vapor and an estimated one percent level of oxygen during the end of a normal charge period.

It is known that the presence of oxygen will tend to deactivate any activated metal hydride and reduce its hydrogen capacity. However in several feasible designs it is possible to restrict oxygen from contact with the hydride. But keeping the water vapor in the battery away from the hydride is virtually impossible without elaborate procedures. Therefore for any of the hydride candidates to perform successfully in a battery, they must perform in the presence of water vapor.

The hydride material most suitable for operation under these conditions is lanthanum pentanickel. Vanadium, columbium, and iron-titanium hydride degrade rapidly in hydrogen capacity in the presence of water vapor.

Tests in the wet hydrogen cycler (room temperature i.e. saturated hydrogen) confirm the information in the literature about the rapid deactivation of vanadium and columbium. ([4]) Within five to ten cycles of wet hydrogen up-take and release the capacity dimished by at least ninety percent. On the other hand, lanthanium pentanickel showed a fifty percent capacity reduction only after 2100 cycles.

The available samples of iron-titanium were not successfully activated to their fully hydrided state of approximately two atoms of hydrogen per one iron-titanium pair. Only about 1.2 atoms of hydrogen was obtained. Under this incomplete hydrided state and coupled with literature indications that suggests that iron-titanium is as sensitive to water presence as is vanadium and columbium, ([6]) the iron-titanium was not completely characterized.

Henceforth the study concentrated on various aspects of performance of lanthanium pentanickel hydride as the material for possible reservoir use in metal-hydrogen batteries.

b. Hydrogen Cycling Study

The lanthanum pentanickel hydride is seen as the only hydride material at the present time capable of sustained performance in a metal-hydrogen battery system.

The results of the cycling performance of five grams of lanthanum pentanickel in the 2 amp-hour nickel-hydrogen battery is

shown in Figure 3. The pressure in the 82cc void volume container upon charge shows a plateau at 3.75×10^5 pascals (3.7 atm). Without any hydride in the container, the pressure would rise to 1.825×10^6 pascals (18 atm) upon charge completion. As the cycles of charge and discharge progressed, the end-of-charge pressure increased. This indicates a cummulative deactivation of the hydride resulting in more hydrogen being stored in the void volume of the container and less and less in the hydride.

The reason for the decay in hydride capacity in the test nickel-hydrogen battery was due to the presence of water vapor and/or oxygen. It is unlikely that the potassium hydroxide electrolyte could have migrated from the cell matrix and through the Teflon films holding the hydride and caused the cummulative decay. Even if liquid electrolyte did reach the Teflon film layer, it is the general experience that without carbon dioxide gas (to form potassium carbonate which acts as a wick that grows through the Teflon pore structure) very little potassium hydroxide can penetrate the Teflon layer.

The sample of hydride in the battery was analyzed for oxygen content after the 120th cycle. The level of oxygen content after 120 cycles analyzed by inert gas fusion techniques was 4.7%. Samples of uncycled hydride analyzed for oxygen yield concentrations from only 130ppm to 0.8%. This points to the fact that oxygen in the battery has a significant effect on the hydride performance. Water vapor or water vapor plus oxygen could also have contributed largely to hydride decay. Therefore, the dry and wet hydrogen cycling tests were established to test this hypothesis.

The results from the dry and wet hydrogen cycling apparatus are shown in Figure 4. The lanthanum pentanickel hydride in the dry cycler showed a 23% reduction in hydrogen capacity at 1000 cycles. In the wet cycler apparatus the capacity was reduced by 39% after 1000 cycles. The vanadium and columbium hydrides decayed practically immediately with wet hydrogen negating their use as reservoirs in metal-hydrogen batteries.

The cycling ability of lanthanum pentanickel increased in the dry and wet hydrogen apparatus over its cycling performance in the nickel-hydrogen 2 Amp-hour test battery by a factor greater than ten. This suggests that oxygen contact in the battery along with control of oxygen levels is an important factor in hydride/battery design.

    c.   P-C-T Equilibrium Study

The equilibrium pressure-composition-temperature relations for lanthanum pentanickel are shown in Figure 5 from 0 to 38°C. These isotherms were obtained by following the incremental decom-
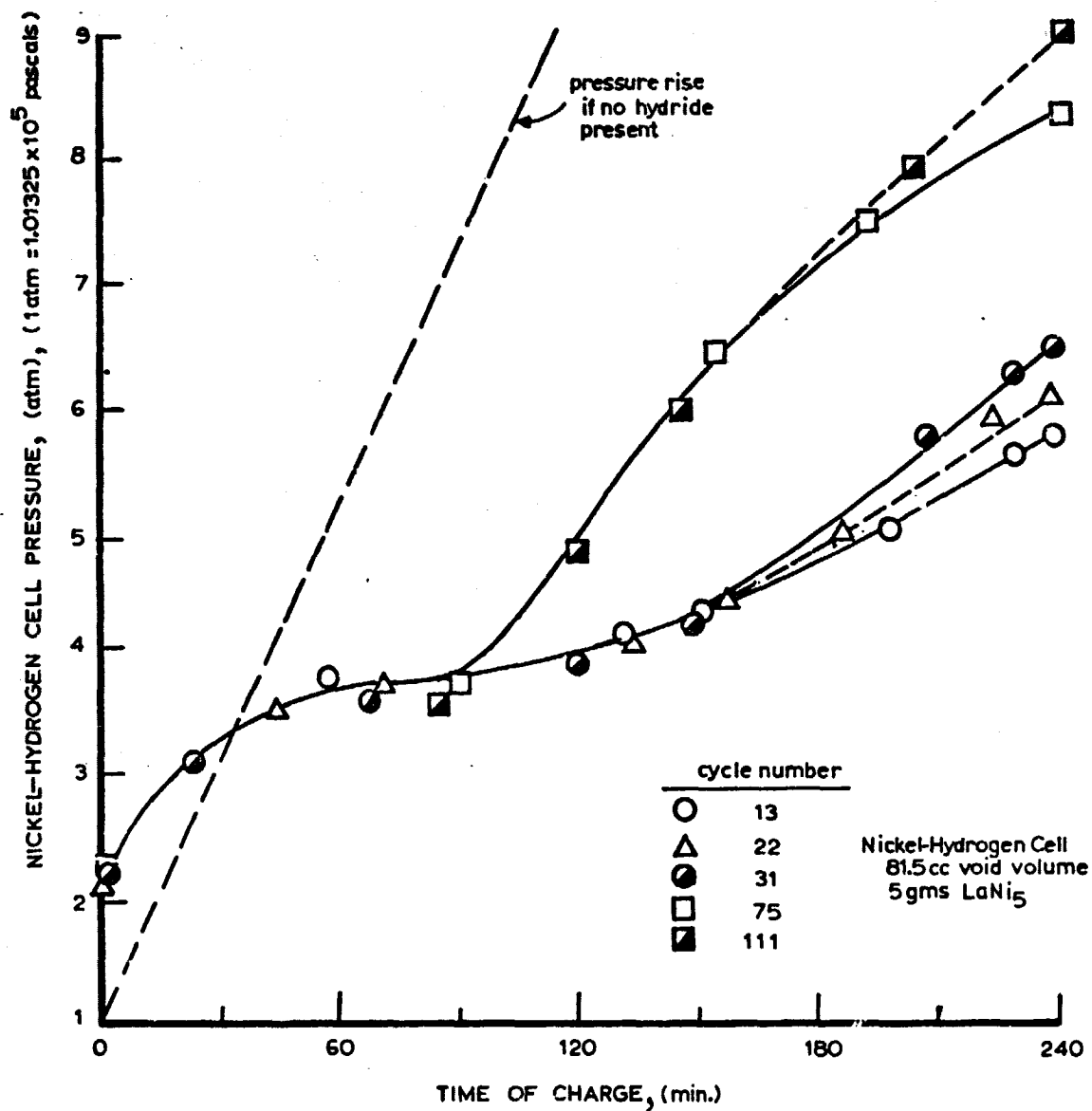
FIGURE 3 CYCLING PERFORMANCE OF LANTHANUM
PENTANICKEL HYDRIDE IN A 2 AMP-HR NICKEL-HYDROGEN TEST CELL
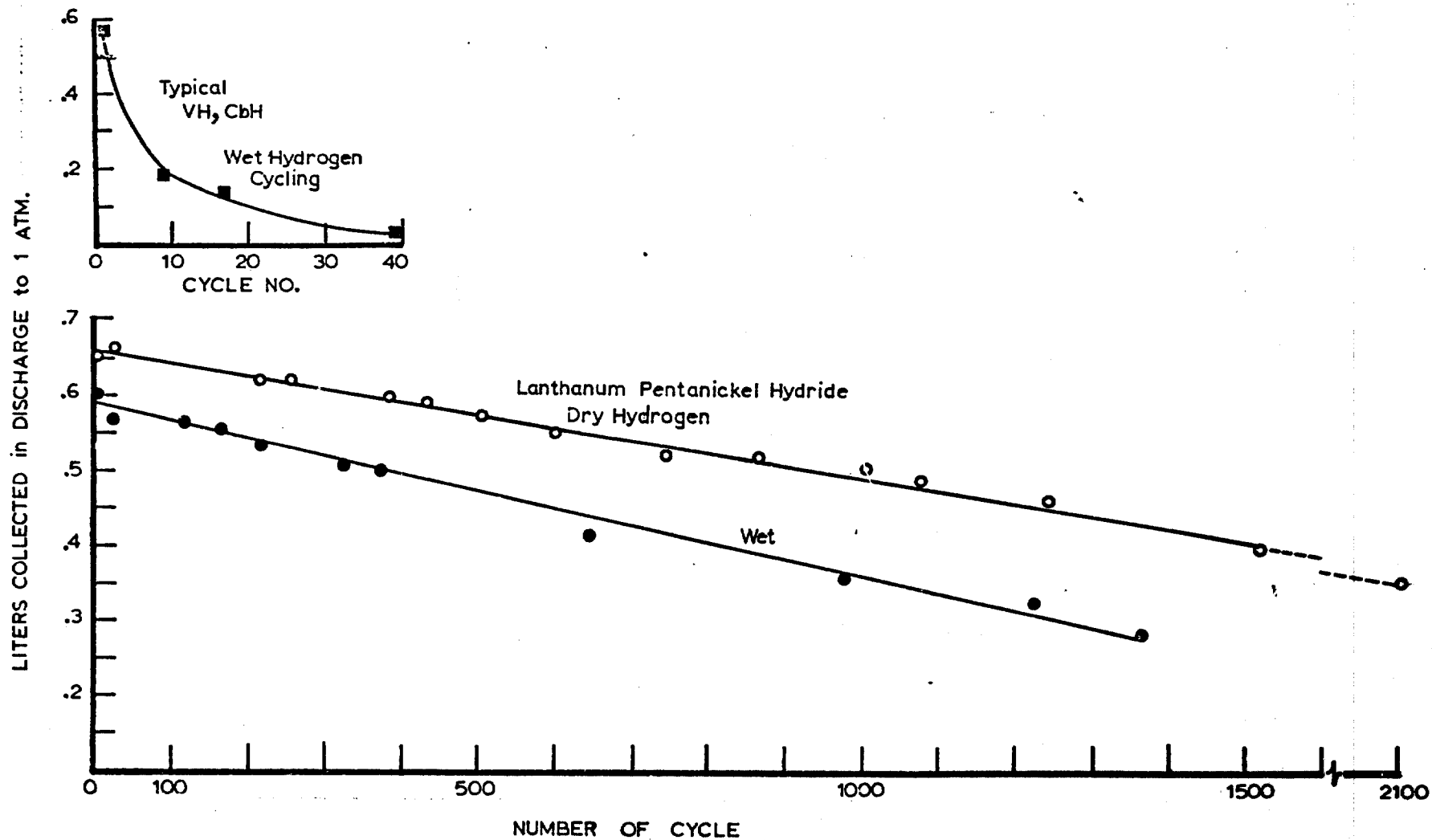
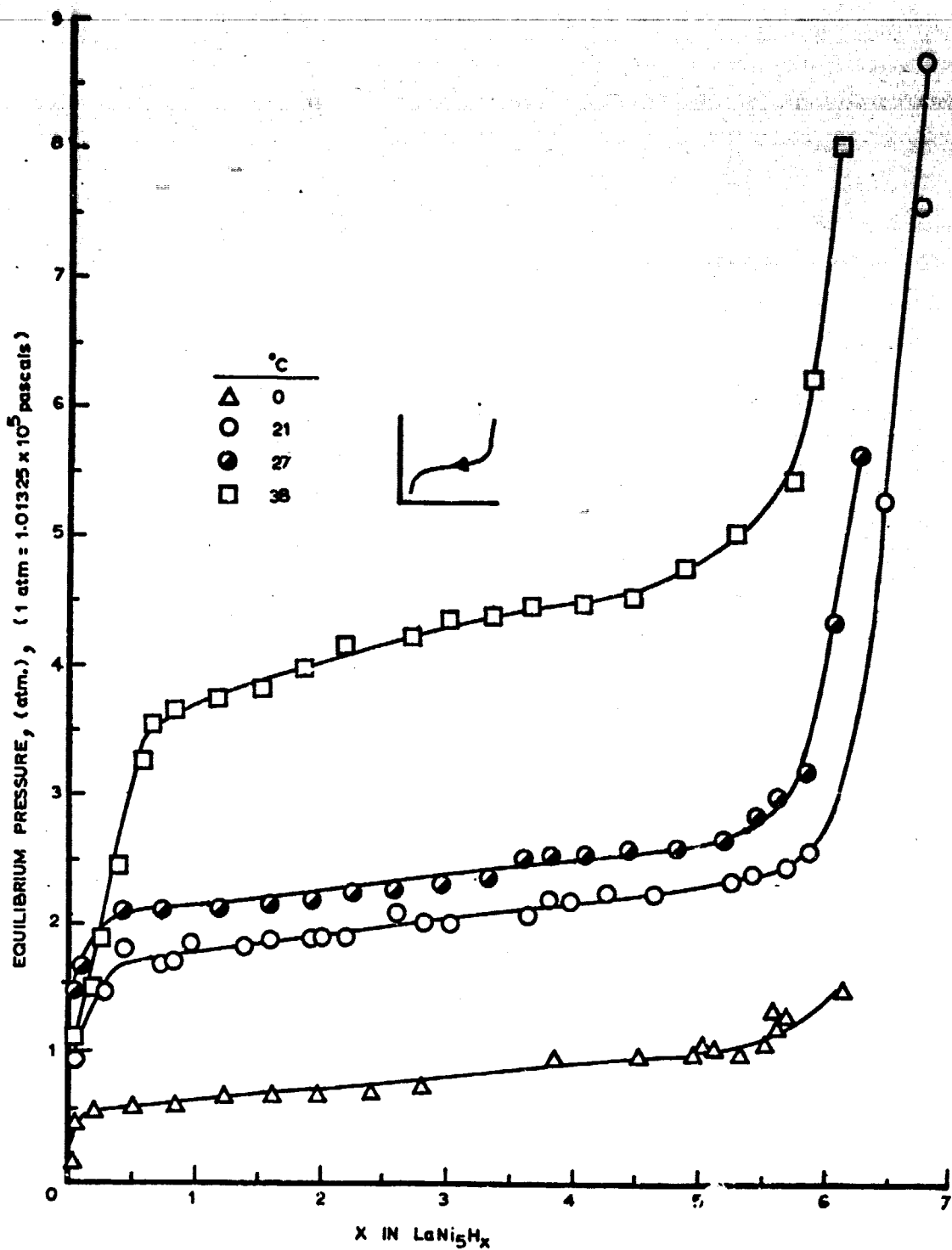FIGURE 4   PERFORMANCE IN DRY AND WET HYDROGEN CYCLING APPARATUS

FIGURE 5   EQUILIBRIUM PRESSURE-COMPOSITION-TEMPERATURE
RELATION FOR LANTHANUM PENTANICKEL

position of the hydride from its fully hydrided state.

The behavior and pressure levels confirm within 10% the isotherms present in the literature.[8] The 0°C isotherm is new information however, and it shows an equilibrium pressure plateau level from below 1.0×10^5 pascals (1 atm) to about half that value.

Isotherms taken in the reverse direction (i.e., formation of the hydride) shows in the literature [8] slightly higher pressure plateaus (as a hysterisis behavior). But for the battery application of interest, the discharge or hydrogen-release situation is more important for design purposes. The reason for this is that the time available in a probably mission cycle for charging (hydride formation) usually substantially exceeds the discharge time. Hence the formation of the hydride at a sligntly higher pressure which results in an identical fully hydrided end point with respect to pressure is not an important performance characteristic. The shorter discharge time behavior characteristics would be controlling in the system design.

d. Hydride Decomposition Rate Study

The rate at which hydrogen is released by the hydride is crucially important in design of hydride materials in metal-hydrogen batteries. The knowledge of the dependence of this hydride decomposition rate upon temperature and the hydrogen backpressure is necessary.

The hydride formation rate though important is not critical with respect to the metal-hydrogen battery mission operation as the charge or formation time is greater than the discharge time. The battery system design is controlled mainly by its discharge characteristics.

The measured isothermal rate of hydride decomposition at various temperatures is presented in Figure 6. This rate is nearly the intrinsic decomposition rate as is explained later. It is presented as (cc of hydrogen at STP per minute per gram of lanthanum pentanickel). The rate is scaled to the amount of lanthanum pentanickel as is generally the case in gas-solid reactions with consumable solids (in this case the hydrided metal portion of the lanthanum pentanickel). Also the rate is plotted against hydride composition which shows the natural decline in rate as the hydride depletes.

In kinetic studies it is more conventional to plot rate against time rather than against composition. But measuring rate directly and continuously with time is extremely difficult because the temperature drops severely. Maintaining isothermal conditions
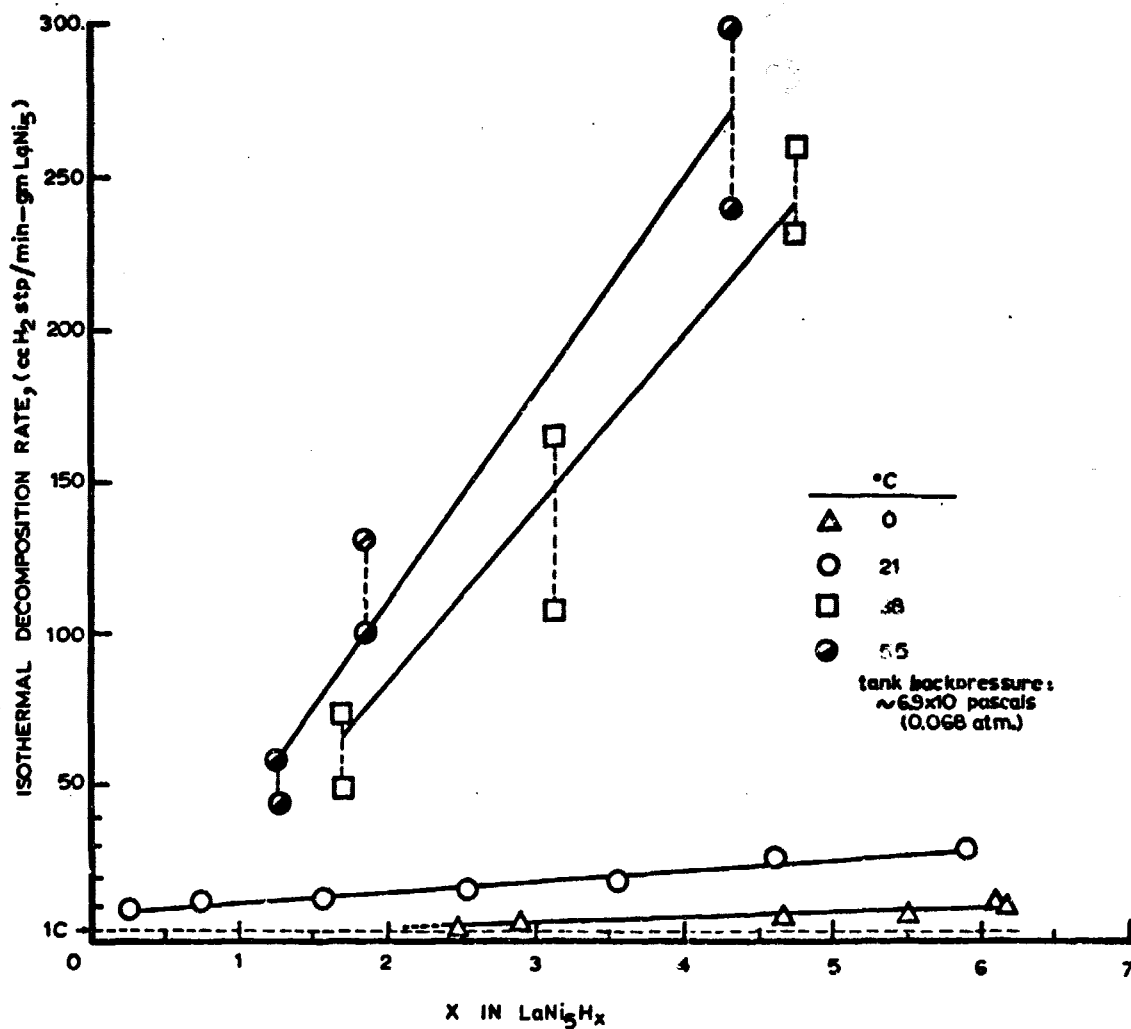
17

FIGURE 6   DECOMPOSITION RATE OF LANTHANUM PENTANICKEL
HYDRIDE AT VARIOUS TEMPERATURES

would have required complicated procedures. However, an indirect method (which will be discussed later) was devised to construct the more conventional rate versus time discharge plots which are useful in kinetic studies.

The values of the discharge or hydride decomposition rate at probable battery operating temperatures between about 25°C and down to 0°C exceed the battery demand rate which is given as the "1C" rate point, about 3.4cc hydrogen per min. per gram lanthanum pentanickel. The "C" rate for battery discussion purposes is that rate at which all the energy stored in any given battery is taken out in one hour. As is shown in Figure 6, at 38 and 55°C, where the discharge rates are very high, the measurement error becomes quite large. The difficulty was with the limit of the apparatus measuring these extremely high values which were about 100 times the 1C rate.

The rates plotted in Figure 6 are nearly the maximum intrinsic rate of decomposition. The near vacuum conditions (0.07 atm) in the mole measuring tank have an immeasurable backpressure "suppressing" effect on the intrinsic decomposition rate.

In Figure 7 the hydride decomposition rates are shown for various tank backpressures at 21°C which significently reduce the intrinsic decomposition rate. Knowledge of this behavior is necessary for battery design as the normal operating hydrogen pressure in the battery is certainly above vacuum conditions until possibly the end of discharge when nearly all the hydrogen could be depleted. The behavior represented in Figure 7 is also helpful in interpreting and describing the kinetic behavior in terms of a model.

As previously mentioned, experimental attempts to directly measure isothermal rates of decomposition in time have not been completely successful without complicated precautions. Generally, isobaric measurements are made rather than isothermal measurements. The method developed in this study of incrementally measuring the rate in short time discharges maintains isothermal conditions, but the time of discharge disappears from the direct data. Hence this is the reason for plotting rate against composition, which for battery evaluation purposes is immediately useful. However, for kinetic studies, rate against time is more conventional. But the two approaches or plots are equivalent.

The rate versus time plot is constructed and shown in Figure 8. The plot was constructed by dividing the rates in Figure 6 into small increments of hydride composition. In each increment the rate is then taken as an averaged constant valve and the amount of hydrogen in that increment is known. The division of the incremental hydrogen amount by the average rate yields the
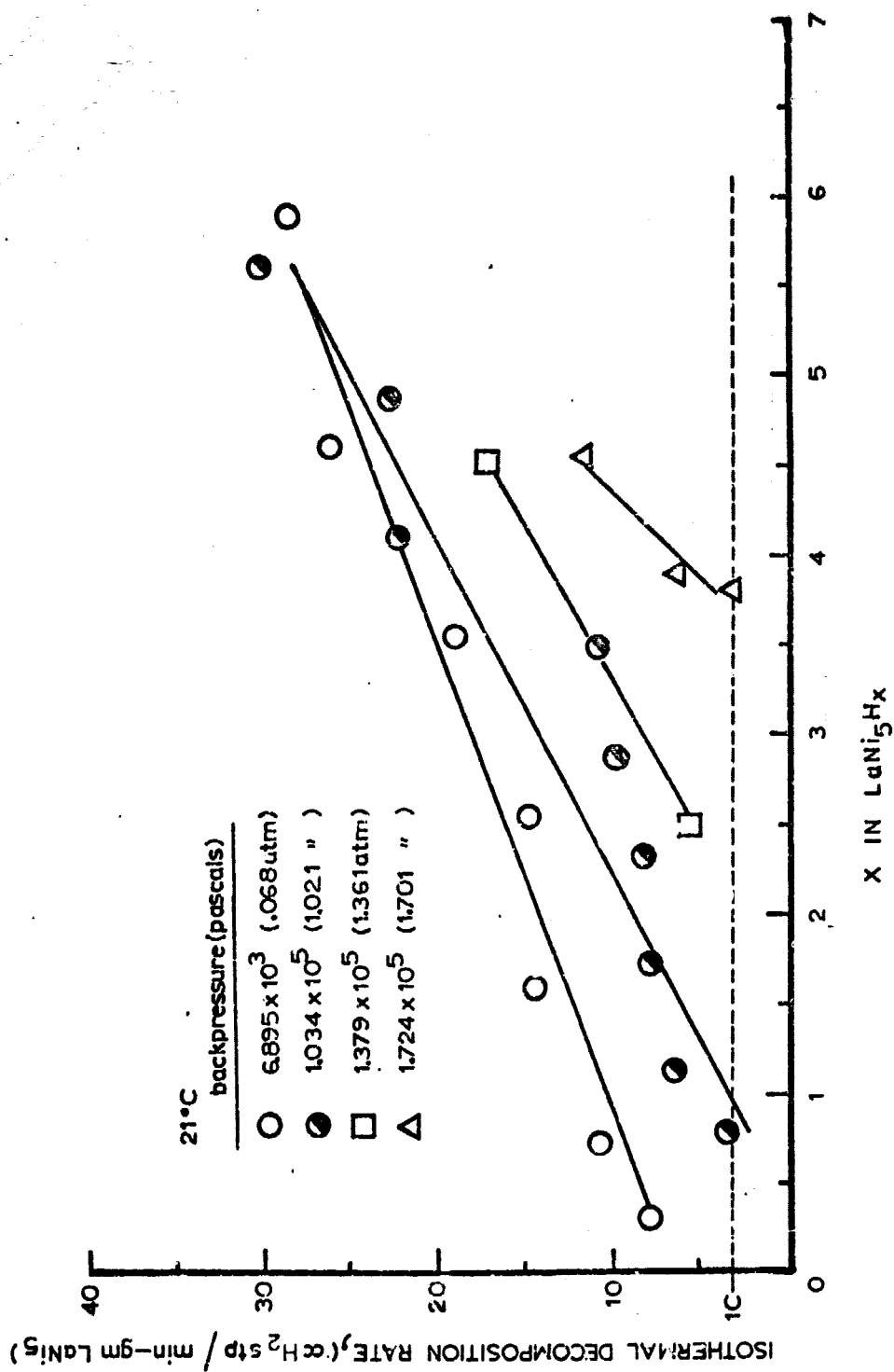
19

FIGURE 7   DECOMPOSITION RATE OF LANTHANUM PENTANICKEL HYDRIDE
AT VARIOUS BACKPRESSURES

time point associated with that rate value. The horizontal lines in Figure 8 represent that averaged rate value over the increment of time. An approximate straight line was drawn to envision the behavior and yield an approximate slope. By taking more and smaller increments in Figure 6 (ideally aided by a computer) a smoother plot could be made. The equivalence of the two plots of rate are shown later in the section on the kinetic model.

e. Heat of Reaction and Energy of Activation

From the lanthanum pentanickel rate data, the values of rate constant, energy of activation, and heat of the decomposition reaction were estimated. The values derived from the results of the present data compare well with the literature values.

The rate constants agree closely with what is available and are discussed in the next section. The energy of activation was estimated assuming an Arrhenius type relation for the rate constant as $11.4 kcal/gmole$ H_2 which compares well with $12 kcal/gmole$ H_2 in the literature.[7]

The heat of decomposition reaction given in the literature ([5],[8]) for lanthanum pentanickel at 25°C is $7 - 7.6$ $kcal/gmole$ H_2. The calculated value from the equilibrium data using the van Hoff relation is 7.9 $kcal/gmole$ H_2.

5. DESCRIPTION MODELING FOR SYSTEM DESIGN

1. Decomposition Rate Model for Lanthanum Pentanickel

The decomposition rate of lanthanum pentanickel hydride as shown in Figures 6 and 7 is a function of the hydride concentration, the pressure of hydrogen, and temperature. First attempts in the literature ([9]) ascribed a first order rate dependence with hydride concentration and a linear dependance on the difference between equilibrium pressure and backpressure. This approach is in the right direction but it does not completely explain the data because it neglects the backward rate of hydrogen sorption.

That first model predicts a decrease in the slope of the rate (plotted against hydride concentration) with an increase in the backpressure. The data in Figure 7 shows an increase in slope with an increase in backpressure.

A model was developed in this study that better expresses the behavior of the data. The expression of the decomposition rate is derived from a combination of a "forward" rate for hy-
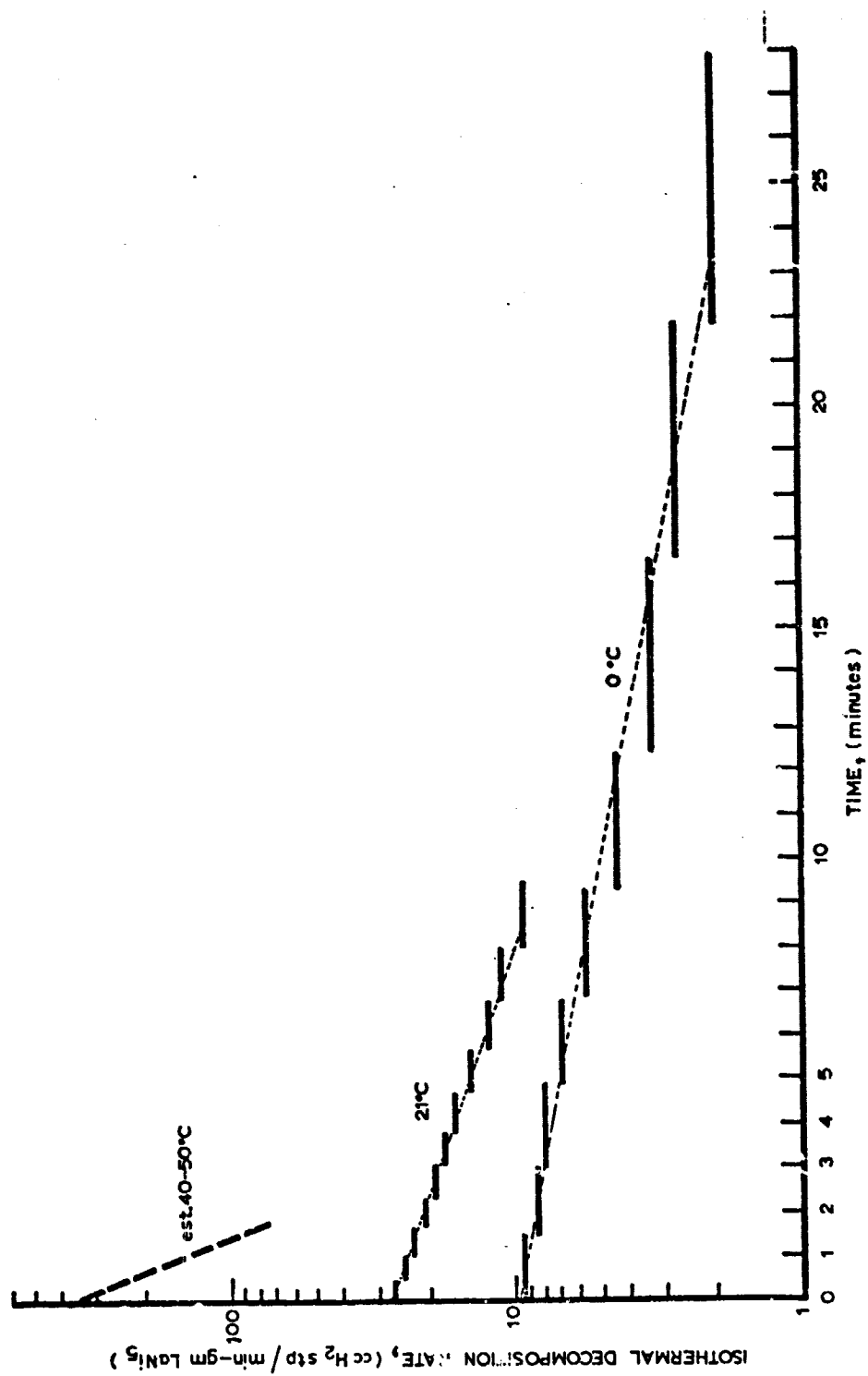
FIGURE 8   CONSTRUCTED RATE VERSUS TIME AT VARIOUS TEMPERATURES

22

dride decomposition and a "backward" rate for hydride formation.
The forward rate is assumed to have a first order dependance on
hydride concentration and the backward rate is dependent on hy-
drogen backpressure and a metal (non-hydride) concentration. The
hydride and metal concentrations are related through stoichiometry.

The difference between these two rates expresses a net rate
of decomposition. This is the rate that is measured experimen-
tally assuming isothermal conditions and no significant mass
transfer limitations in the measurement.

Hence,

[net rate of decomposition] =

[hydride decomposition rate] - [hydride formation rate]

By the law of mass action, the measured rate is expressed as

$$R = k_d [H] - k_h P_{H_2} [M] \qquad \text{Eq. (1)}$$

where

k_d and k_h are the rate constants for the forward (decom-
position) rate and the backward (hydriding) rate,

[H] is the hydride concentration (related to x commonly

used for the hydrogen atom number in the hydride formu-

la),

[M] is a metal (non-hydrided) concentration, and

P_{H_2} is the hydrogen backpressure.

By a mass balance on the solid material at any time,

$$[H] + [M] = C_0 \qquad \text{Eq. (2)}$$

where

[H] and [M] are related to volume fractions for the

material present and

C_0 is some initial concentration

Typically for a fully hydrided lanthanum pentanickel sample
at room temperature, C_0 is related to the hydrogen atom number of
6.7 (i.e., fully hydrided state). Unfortunately the molar vol-
umes of the compound and solid solutions are not known precisely.

23

Also, if some additional material behaves as an inert component it should be accounted for in Equation (2).

Now eliminating [M] from Equation (1) using Equation (2) yields

$$R = (k_d + k_h P_{H_2}) [H] - k_h C_0 P_{H_2} \qquad \text{Eq. (3)}$$

The expressed rate, R, agrees qualitatively with the lanthanum pentanickel decomposition data at 21°C at various backpressures as presented in Figure 7.

The [H] axis intercept (or x axis for $LaNi_5H_x$) would increase with increasing backpressure as the data in Figure 7 shows and Equation (3) predicts. The slope of the rate versus hydride composition also increases with the hydrogen backpressure.

From zero backpressure data or approximately from the near zero backpressure data in Figure 7 the value of k_d can be obtained as simply the slope. The value of k_h can be determined from the slope of the higher backpressure data using the value determined for k_d and the relation

$$k_d + k_h P_{H_2} = \text{slope} \qquad \text{Eq. (4)}$$

A value for the first order forward rate constant was obtained from the data in Figure 7 in this manner. The value of k_d was 0.14 min^{-1} at 21°C. This compares closely to available data on lanthanum pentanickel[8]. That data is not isothermal, but isobaric; however, for very short times the data is approximately isothermal and yields a value for the forward rate constant as approximately 0.1 min^{-1}.

The constructed rate versus time plot in Figure 8 also yields the same value for the forward rate constant. This shows the equivalence of Figure 7 and Figure 8, the more conventional method of plotting gas-solid rate behavior.

The value of the backward rate constant obtained is not constant for the three backpressures of the data in Figure 7. Two of the three values are very close. To obtain a better estimate of k_h from the data using the model requires more refined experimentation than was accomplished in this initial investigation.

However, an attempt was made to fit the rate data at 21°C and various backpressures to the model. The results are shown in Figure 9 for (1), (the solid lines) the case where the constants in Equation (3), namely k_h, k_d, C_0 are taken as the best estimates given by the data; and (2), (the dotted lines) the case
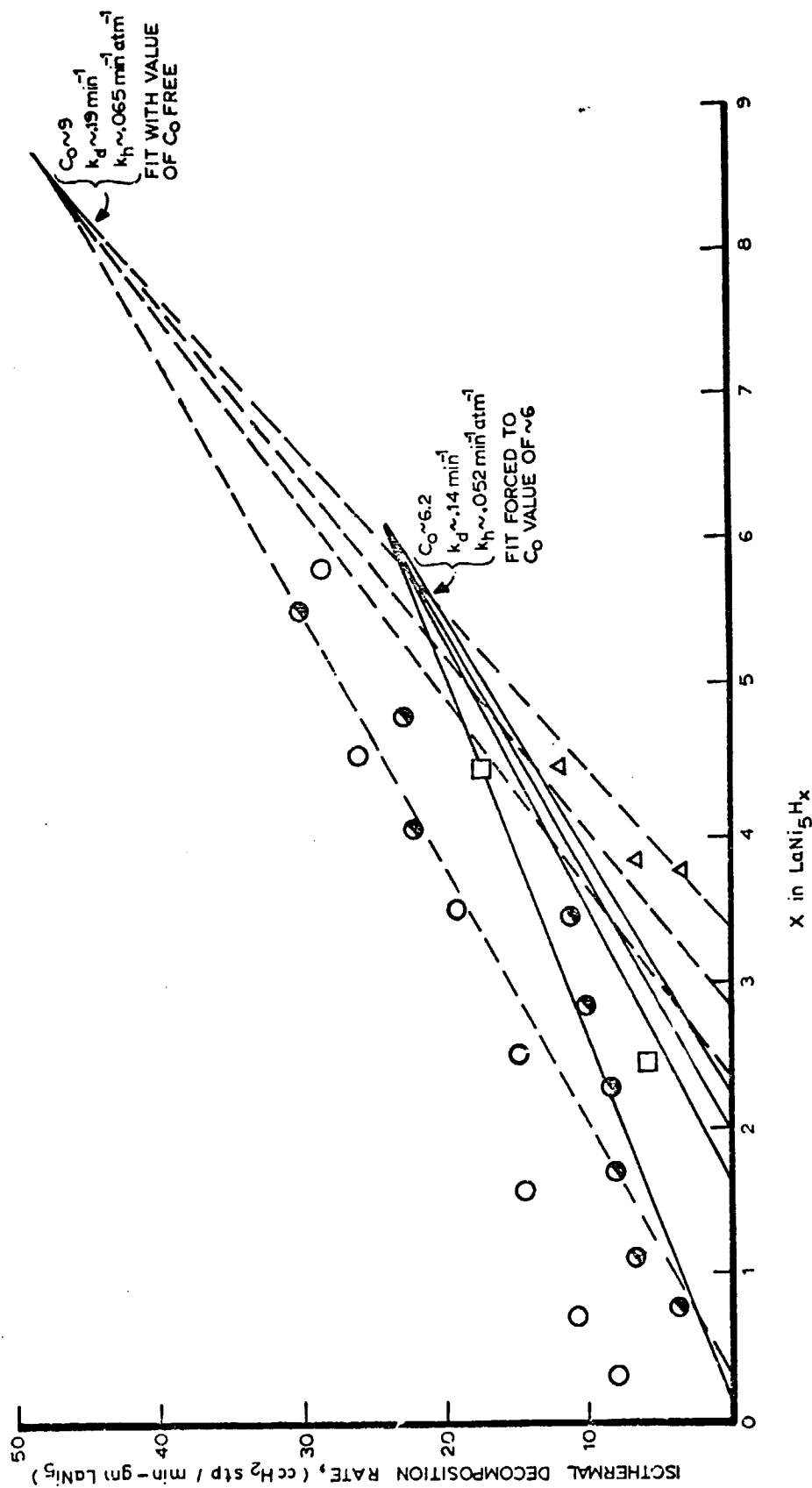
24

FIGURE 9   EXPERIMENTAL RATE DATA AND HYDRIDE REACTION MODEL BEHAVIOR FOR VARIOUS BACKPRESSURES

25

where the parameter values k_h, k_d, C_o were changed arbitrarily to produce the best coincidence with the data. The fit in either case is limited. The solid and dotted lines do in a manner enclose the data, suggesting qualitatively the correct behavior.

The questions raised by the quantitative determination attempt in Figure 9 are interesting. The model may predict that the observed 6.7 atoms of hydrogen per lanthanum pentanickel may not be the maximum theoretical value. There are some ideas that 6.7 atoms of hydrogen possibly may not be a maximum theoretical value for lanthanum pentanickel, such as the free fit in Figure 9 suggests with its value of approximately 9 atoms of hydrogen. This aspect is quite speculative at this point, but it is not unreasonable.

The analysis depicted in Figure 9 would be enhanced if the model considered the change in volume that occurs during hydride formation and decomposition. The 25% volume change is significant but was neglected in the initial model development. Additional model investigation and experimentation is required to clarify these points.

Another interesting and important result is obtained when the model rate expression, i.e. Eq. (1) is set equal to zero. Zero rate implies equilibrium and the resultant expression generally predicts the equilibrium pressure-composition isotherms' shape.

Setting R = 0 in Eq. (1) and using Eq. (2) yields

$$(P_{H_2})_{eq} = \left(\frac{k_d}{k_h}\right)\frac{[H]_{eq}}{[M]_{eq}} = \left(\frac{k_d}{k_h}\right)\frac{[H]_{eq}}{[C_0^- [H]_{eq}]} \qquad \text{Eq. (5)}$$

In Equation (5), thinking of $(P_{H_2})_{eq}$, $[H]_{eq}$, and $[M]_{eq}$, as variables (at constant temperature) yields qualitatively the observed isotherms' shape.

Furthermore, if the shape of the equilibrium pressure-composition isotherm (as in Figure 5) is considered to be the sum of a base compound pressure and the pressure given by Eq. (5), then the following expression results.

(measured equilibrium pressure) =

$[Pcompound]_{eq} + [P_{H_2}]_{eq} =$

$$[Pcompound]_{eq} + \left(\frac{k_d}{k_h}\right)\frac{[H]_{eq}}{[C_0^- [H]_{eq}]} \qquad \text{Eq. (6)}$$

26

Eq. (6) does have the necessary elements to produce the approximate form of the measured isotherms. The pressure tends to become infinite when $[H]_{eq} = C_o$ as the isotherms tend to show. And depending on the magnitude of the terms in the ratio in Eq. (6), a plateau region could be described. This is still a tentative point in the overall application of this model.

2.   Thermal Analysis of Hydride/Battery Integration

The hydrogen production in any system utilizing metal hydrides is greatly dependent upon temperature. This section presents the analysis of the thermal energy balance between the metal hydride and the metal-hydrogen battery held in close proximity in the same container. Proper analysis is needed for this system mainly because the heat available from the battery to the hydride is not present in a large excess.
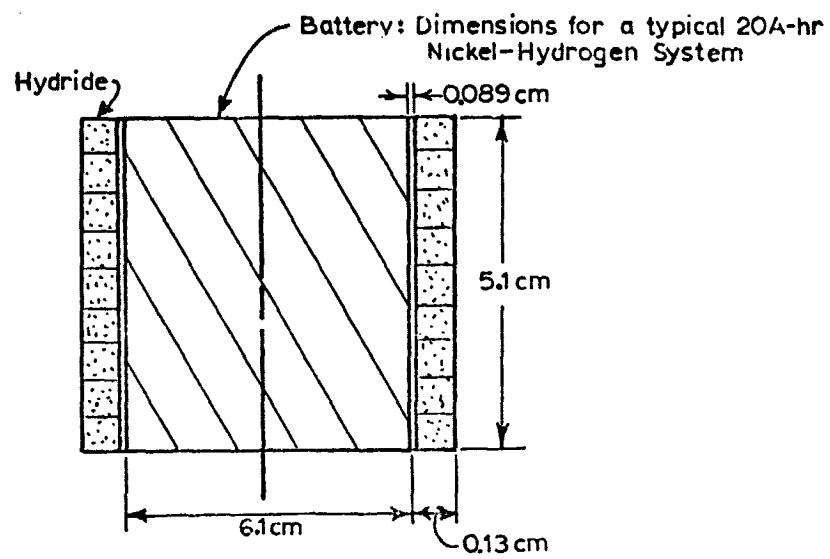
If it were not for oxygen contamination of the activated metal hydrides, the most desirable place in terms of heat transfer to have the metal hydride would be between the electrodes of the nickel-hydrogen battery. This would represent a space and thermal energy efficient design. However there is no practical way to prevent the very small levels of oxygen from contacting the sandwiched hydride layers.

Therefore two other possible designs are considered that place the hydride in good thermal proximity but allow some method of oxygen control. These possible arrangements of the hydride are shown in Figure 10.
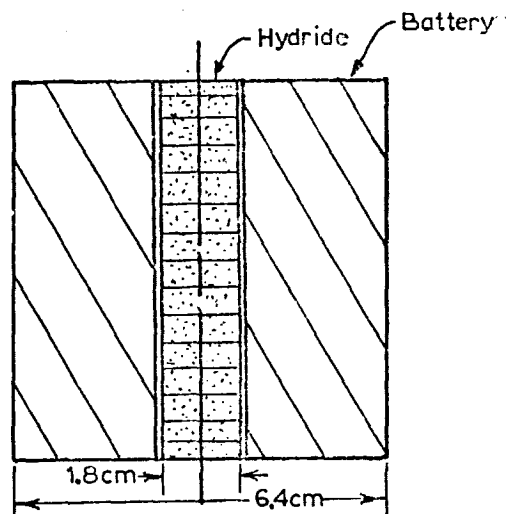
Case I shows the hydride contained in a very thin annular region about the cylindrical battery stack. In case II, the hydride is held in a thin wall tube positioned down the center of the stack. Each of these cases is analyzed considering unsteady state heat conduction from the heat source of the electrodes to the heat sink of the hydride during the time of discharge of the battery. The detailed analysis for each case is presented in Appendix 2.

The resultant governing equations were applied to a typical 20 amp-hour nickel-hydrogen battery. The hydride property values were taken for lanthanum pentanickel hydride; also the system was applied to show how a hydride with a heat of reaction twice that of lanthanum pentanickel would behave in the battery system. The results of the analysis are shown in Figure 11 as hydride temperature change during the battery's discharge period.

3.   Design Recommendations for Integrated Hydride/Battery
      Systems

CASE I: METAL HYDRIDE in ANNULAR REGION

Battery: Dimensions for a typical 20A-hr Nickel-Hydrogen System

Hydride

0.089 cm

5.1 cm

6.1 cm

0.13 cm

CASE II: METAL HYDRIDE in CENTER of BATTERY

Hydride   Battery

1.8 cm

6.4 cm

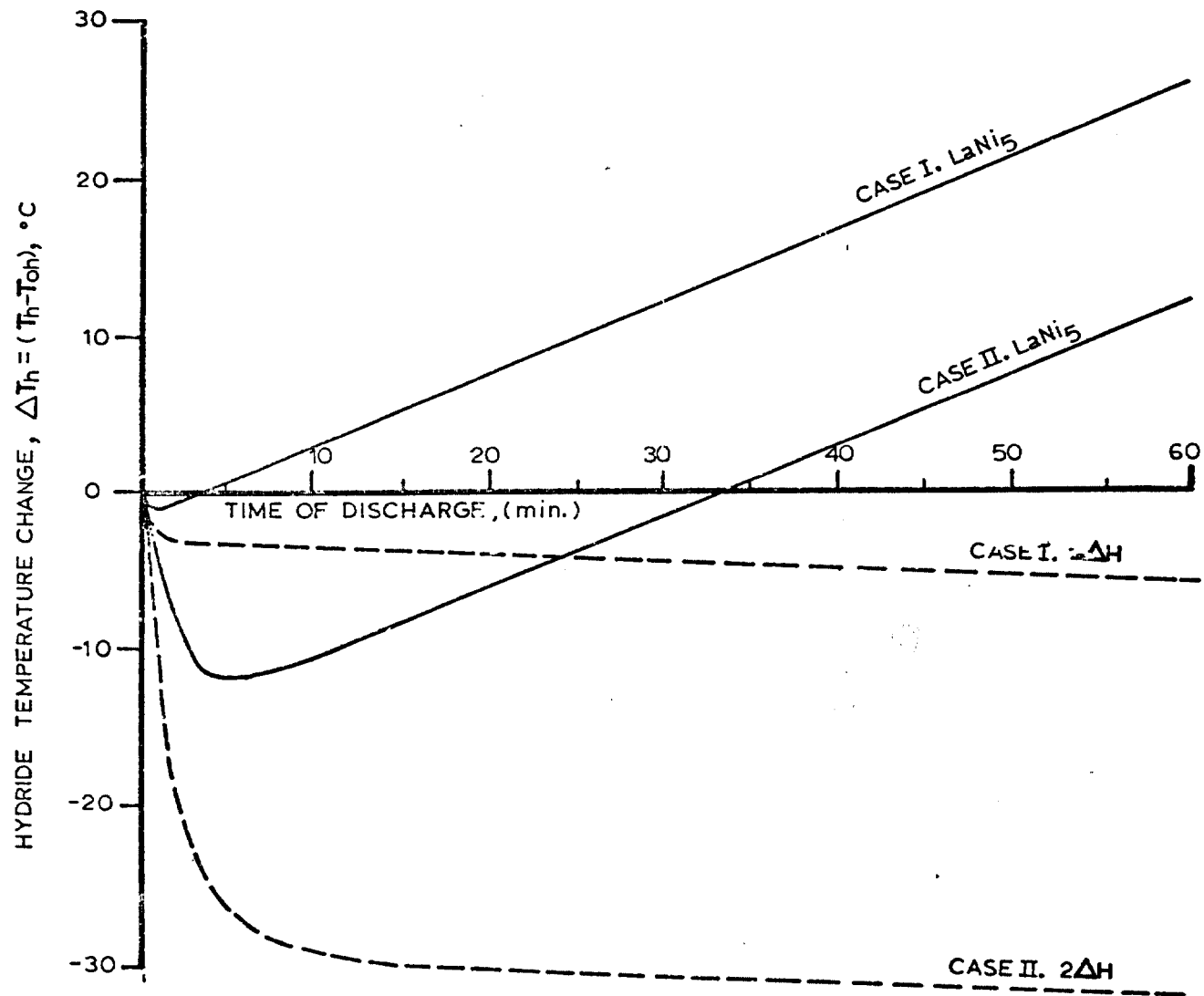FIGURE 10   METAL HYDRIDE-BATTERY INTEGRATION

28

FIGURE 11   METAL HYDRIDE TEMPERATURE PROFILES DURING DISCHARGE

The lanthanum pentanickel hydride could perform successfully from a thermal point of view in the battery system when positioned either as in Case I or Case II.

Whether or not a hydride with a heat of reaction twice as great as lanthanum pentanickel would work satisfactorily in either case depends on the hydride's starting temperature and its rate of hydrogen supply at that temperature.

The hydride's starting temperature could be high enough such that any temperature drop that occurs would result in lowered temperatures but still high enough that the hydride can supply hydrogen at sufficient rates at these lowered temperatures. For example, as seen in Figure 11, Case II, lanthanum pentanickel hydride could start producing hydrogen at 10°C and after five minutes its temperature would be near 0°C. At 0°C its decomposition rate is still above the 1C battery rate as shown in Figure 6.

Lanthanum pentanickel appears as the best material to be chosen for integration in metal-hydrogen batteries considering its thermal behavior, sufficient hydrogen supply rates, a¹ apparent tolerance to the battery environment.

6. CONCLUSIONS

The performance characterization shows that lanthanum pentanickel can operate in the battery environment. Contact with low concentration oxygen can be avoided by certain design modifications, for example with catalytic conversion of oxygen on platinum black. The other materials, vanadium, columbium, and iron titanium are unlikely candidates because they exhibit poor tolerance to the presence of water vapor which will always be present in aerospace type metal-hydrogen batteries. For very large metal-hydrogen battery systems as might be used in load leveling special provisions for water removal and hydride isolation might be feasible.

The hydrogen supply rate from the decomposition of lanthanum pentanickel hydride is sufficient for metal-hydrogen battery operation in the 0-50°C temperature range. The hydrogen capacity and cycling behavior of lanthanum pentanickel is confirmed. A hydride/battery integration seems feasible. The heat of reaction, energy of activation, and an estimate of the decomposition rate constant have been obtained and confirmed with literature values.

Analysis of the thermal behavior of lanthanum pentanickel positioned in a possible battery arrangement indicates that the heat balances are favorable for operation.

30

A model that involves the kinetic behavior of the lanthanum pentanickel hydride decomposition has been formulated. The qualitative fit of the model to the data is excellent. All the important observations of hydride decomposition are accounted and the model yields (within experimental error) a constant decomposition rate constant. The reduction of the measured rate by backpressure is also predicted.

Extending this model to data at various temperatures and refining the data acquisition will result in excellent understanding of lanthanum pentanickel hydride behavior as well as other hydride materials.

The possibility also exists that hydride forming materials that perform as well or better than lanthanum pentanickel may still be discovered.

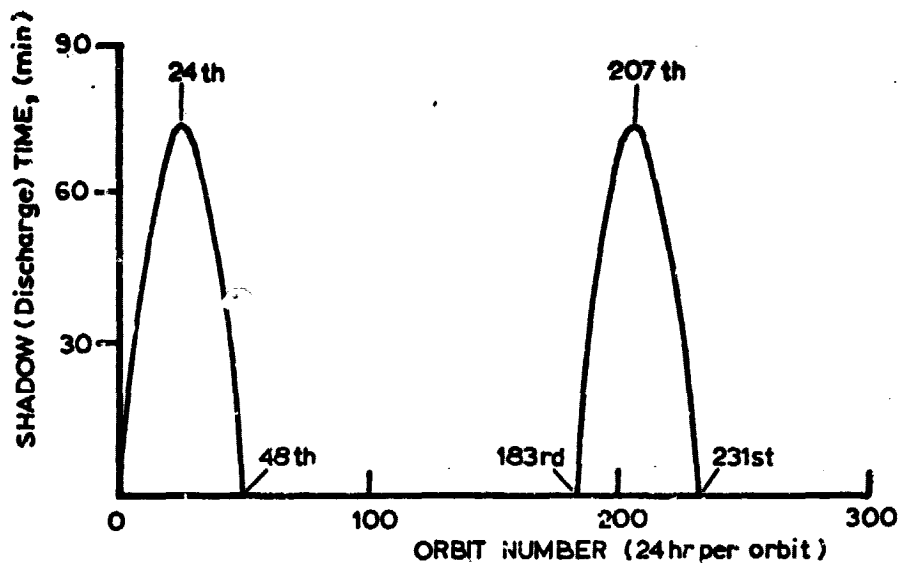APPENDIX I

Typical Battery Orbit Duty

FIGURE 12. TYPICAL BATTERY ORBIT DUTY

Each orbit is 24 hr. in length, and the cells are alternately charged and discharged for a total of 48 cycles. The discharge period ranges from zero on the first cycle to a maximum of 74 min on the 24th cycle and returns to zero on the 48th cycle in such a manner that the discharge time, as a function of cycle number, approximates a sinusoidal function. Upon completion of these 48 cycles, the battery sees a 135 day wet-stand period after which the 48-cycle discharge routine is repeated.

APPENDIX II

Thermal Analysis of Metal Hydride/Metal Hydrogen

Battery Integration

Case I - Metal Hydride in Annular Region (see Figure 9)

Governing Equations:

$$M_h C_{ph} \frac{dT_h}{dt} = UA(T_b - T_h) - Q_1 \qquad \text{Eq. (7)}$$

$$M_b C_{pb} \frac{dT_b}{dt} = UA(T_h - T_b) - Q_2 \qquad \text{Eq. (8)}$$

where

$M_{h,b}$ = weight of hydride, battery

$C_{ph,b}$ = specific heat of hydride, battery

$T_{h,b}$ = temperature of hydride, battery

U = heat transfer coefficient

A = heat transfer area

Q_1 = heat of desorption of hydrogen

Q_2 = heat generated by battery, discharge

t = time

and initial conditions,

$T_h(t=o) = T_{oh}$ = initial hydride temperature

$T_b(t=o) = T_{ob}$ = initial battery temperature

The analytical solution can be obtained either by simultaneous first order differential equation methods or by LaPlace transforms.

The analytical solution for the hydride temperature is:

$$T_h = A_1 + A_2 \cdot \exp\left[(h_h - h_b)t\right] + A_3 t \qquad \text{Eq. (9)}$$

where

$$h_h = \frac{UA}{M_h C_{ph}} \quad , \quad h_b = \frac{UA}{M_b C_{pb}} \quad , \quad Q_h = \frac{Q_1}{M_h C_{ph}} \quad , \quad Q_b = \frac{Q_2}{M_b C_{pb}}$$

35

$$A_1 = \frac{h_b T_{oh} + h_h T_{ob} - Q_h - A_3}{h_h + h_b}$$

$$A_2 = (T_{oh} - A_1), A_3 = \frac{h_h Q_b - h_b Q_h}{h_n + h_b}$$

Case IA: $LaNi_5$

The solution for a lanthanum pentanickel representative hydride upon substituting typical values for the various parameters is given as $\Delta T_h = (T_h - T_{oh})$ in °C.

$$\Delta T_h = -1.55 + 1.55e^{-321t} + 29.14t \qquad \text{Eq. (10)}$$

(ΔT_h in °C, t in hours)

The typical parameter values chosen are as follows; for a 20 amp-hour metal-hydrogen battery.

battery heat generation = 2.163×10^4 J/hr

lanthanum pentanickel hydride endothermic heat of reaction =

1.124×10^4 J/hr (7.2 kcal/amoleH$_2$)

$M_b = 0.318$kg; $M_h = .536$kg

$C_{pb} = 1.047 \times 10$ J/kg·K; $C_{ph} = 4.478 \times 10$ J/kg·K

$k_{H_2} = 6.542 \times 10$ W/m·K

diameter of battery = 6.1cm

height of battery (or hydride) = 5.1cm

width of hydrogen gap = 0.89cm

width of hydride = 0.13cm

36

Case IB: $2\Delta H$

For a representative hydride with twice the heat of reaction, the heat of reaction would be 2.248×10^4 J/hr (14.4 kcal/mole H_2) and the solution becomes,

$$\Delta T = -2.91 + 2.917e^{-321t} - 2.38t \qquad \text{Eq. (11)}$$

Case II - Metal Hydride in Center Position

The temperature in the hydride will not be uniform during discharge in this case. However, we can consider a heat transfer coefficient U with the previous governing equations by lumping the temperature gradient into the heat transfer resistance by considering the steady state heat transfer analysis for the cylindrical section with constant T_b.

The hydride resistance R_h was found to be

$$\frac{r_h}{2k_h} = \frac{\text{radius of hydride section}}{2 \; (\text{thermal conductivity of the hydride})}$$

Hence the overall heat transfer coefficient U, is obtained from

$$\frac{1}{U} = \frac{1}{h_{H_2}} + \frac{r_h}{2k_h}$$

Therefore the previous solution will hold with this value for U and the smaller area A.

Case IIA: $LaNi_5$

The solution for the hydride temperature becomes, for the lanthanum pentanickel heat value,

$$\Delta T_h = -15.52 + 15.56e^{-31.63t} + 29.14t \qquad \text{Eq. (12)}$$

Case IIB: $2\Delta H$

and for the representative hydride double heat of reaction

$$\Delta T_h = -29.55 + 29.55e^{-31.63t} - 2.44t \qquad \text{Eq. (13)}$$

APPENDIX III

Detailed Integration Features of Metal

Hydride/20 A-hr Nickel-Hydrogen Electrode Stack

The following figures illustrate the typical configuration of the integration of a metal-hydride with existing metal-hydrogen batteries such as nickel-hydrogen. The two feasible positions described in the text are shown in more construction detail in Figures 13 and 14, including the positioning of a porous metal catalytic sponge for oxygen control.

These integrations of the metal-hydride with the secondary metal-hydrogen batteries are recommended for construction and testing.
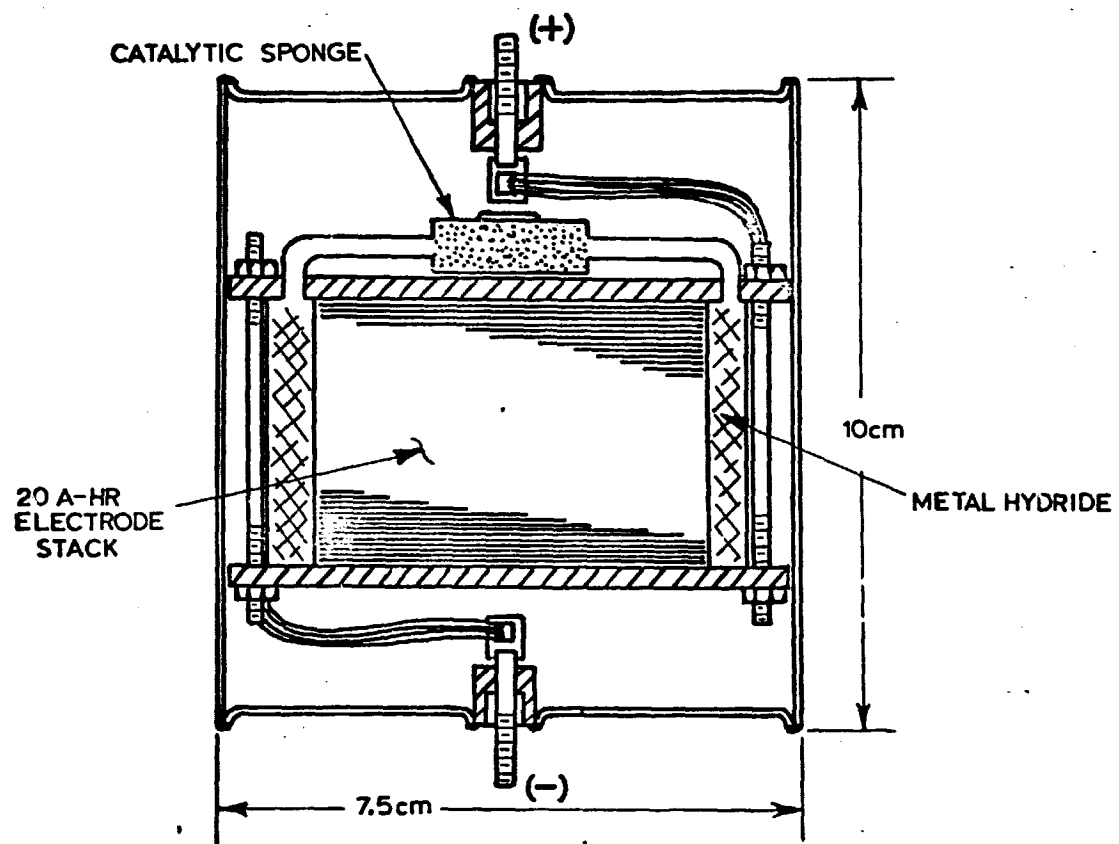
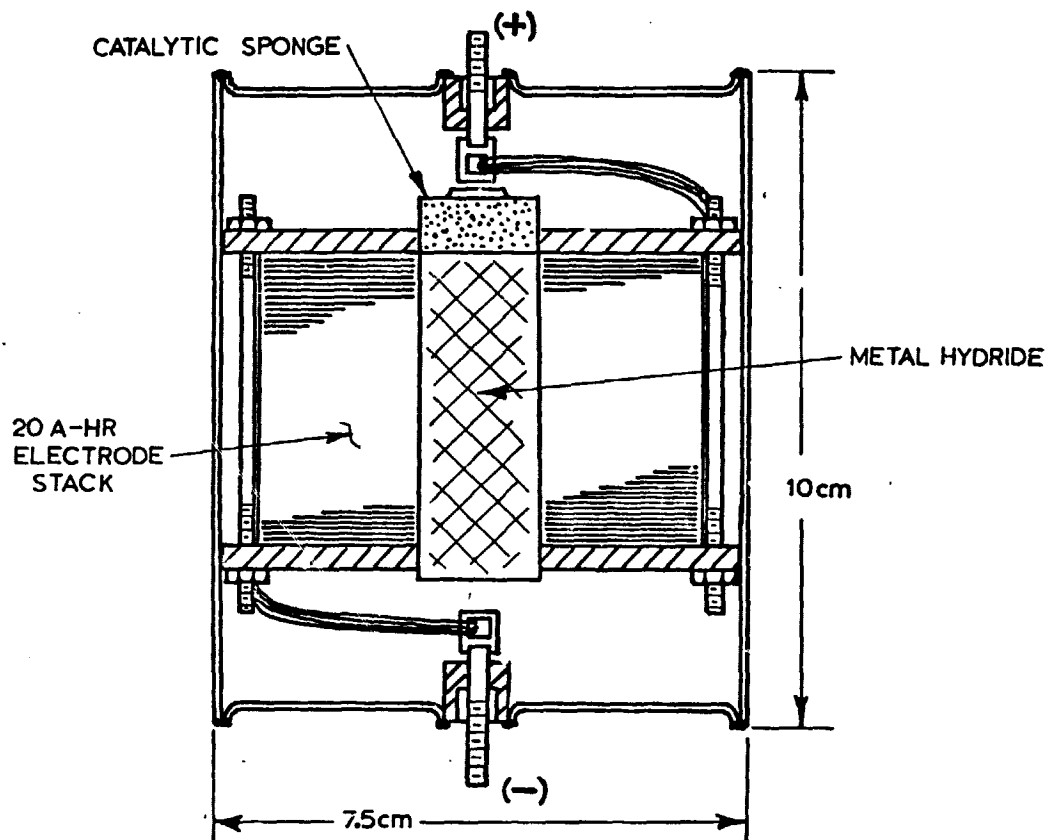FIGURE 13   OUTSIDE ANNULAR HYDRIDE CELL

CATALYTIC SPONGE

(+)

METAL HYDRIDE

20 A-HR
ELECTRODE
STACK

10 cm

7.5 cm

(—)

FIGURE 14   CENTER HYDRIDE POSITION CELL

REFERENCES ·

1. Klein, M. and George, M., "Nickel-Hydrogen Secondary Batteries," 26th Power Sources Symposium Proceedings, pp 18-20, April, 1974.

2. Levy, E. and Rogers, H. H., "Spacecraft Integration and Problem Area Studies on Nickel-Hydrogen Cells," 9th Intersociety Energy Conversion Engineering Conference Proceed⁺ngs, pp 846-854, August, 1974.

3. Klein, M., "Sealed, Rechargeable Silver-Hydrogen Battery," 9th International Power Sources Symposium, pp 347-359, September, 1974.

4. Reilly, J. J. and Wiswall, R. H.,"The Higher Hydrides of Vanadium and Niobium," Inorganic Chem., 9, 1678 (1970).

5. Lehrfeld, D. and Boser, O., "Absorption-Desorption Compressor for Spaceborne-Airborne Cryogenic Refrigerators," Report AFFDL-TR-74-21, Air Force Flight Dynamics Laboratory, Wright-Patterson Air Force Base, March, 1974.

6. Reilly, J. J. and Wiswall, R. H., "The Formation and Properties of Iron-Titanium Hydride," Inorganic Chem. 13, 218 (1974).

7. Lundin, C. E. and Lynch, F.E., "Solid State Hydrogen Storage Materials for Application to Energy Needs," Report to Advanced Research Projects Agency, No AFOSR, F44620-74-C0020, January, 1975.

8. vanVucht, J. H. N., Kuijpers, F. A., and Bruning, H. C. A., Philips Research Reports, 25, 133 (1970). (Philips Laboratories, Division of North American Philips Corp.)

9. Cummings, D. L. and Powers, G. J., "The Storage of Hydrogen as Metal Hydrides," IEC Process Des. Develop., 13, No. 2, (1974).